Proceedings of IMECE2008
2008 ASME International Mechanical Engineering Congress and Exposition
October 31-November 6, 2008, Boston, Massachusetts, USA

IMECE2008-68611

# DEVELOPMENT AND VALIDATION OF A HIGH FIDELITY 3-D COMPUTATIONAL SPINE MODEL THAT INCORPORATES SPATIAL MATERIAL DENSITY VARIATIONS

**Ricardo A. Diaz-Silva, M.S.**
Mechanical and Aeronautical Engineering,
University of California at Davis
Davis, CA, USA

**Nesrin Sarigul-Klijn, Ph.D.***
Mechanical and Aeronautical Engineering,
University of California at Davis
Davis, CA, USA, nsarigulklijn@ucdavis.edu

## ABSTRACT

Anatomically accurate high fidelity computational model of human spine is developed from Computed Tomography scans of a healthy subject and validated against experimental and other computational results.

Procedures developed in this work will serve useful in noninvasive evaluation of patients with back problems. The advantage of this approach is that the model can be tailored to specific individual or specimen

## INTRODUCTION

The present study is novel in that it accurately represents the external geometry, internal architecture and the material distribution of spinal segments based on Computed Tomography (CT) images in a multi-body model, and it validates against experimental values. A full-scale human spinal segment that includes T12 to sacrum is needed for an extensive study of the lumbar spine's mechanical behavior in all degrees of freedom [1]. The soft tissue modeling, in particular the Intervertebral Discs (IVD), represents a challenge in order to incorporate it into the multi-body anatomically accurate lumbar spine model. CT scans based improved modeling approach is utilized for accurate modeling of the discs. The details of full three-dimensional model development as well as the results of the analysis under extension-flexion and torsion loads are given in the following sections.

## MODEL DEVELOPMENT METHODS

### *A. Lumbar spine 3-D geometry modeling*

The geometry of the full-scale lumbar model consisting of T12 to sacrum was obtained based on medical imaging processing from CT scans.

*Corresponding author, copyright owner. Professor and Leader of SpaceED. Member of ASME, nsarigulklijn@ucdavis.edu

The CT images (DICOM file) were of a mature male subject with no apparent bone-related pathologies. The scan had a slice increment of 1.5 mm and slice thickness of 3.0 mm with a resolution of 512 x 512 pixels.

**Figure 1.** Anatomically correct high fidelity model geometry, T12-S vertebral bodies and the discs developed. Standing posture shown.

The first step in the segmentation process using Mimics v10.11 software (from Materialise) was a thresholding of the images identifying minimum and maximum grayscale values (148 and 2054 Hounsfield units respectively). Hounsfield units are the calibrated CT intensity values with HU being zero for water and H being -1000 for air), [2]. This thresholding operation grouped the areas of vertebral bodies plus sacrum in a single mask. While the thresholding was necessary to obtain the areas of interest, the minimum threshold value also resulted in void areas in the cancellous bone. A subsequent region

growing of the selected areas resulted in a mask for each vertebral body. Since sacral vertebrae are fused together, they were treated as one body.

The connected pixels in the mask allowed the software to perform a 3D calculation in which triangular elements formed a shell enclosing the resulting volume. Before exporting the triangular surface mesh for each vertebral body into analysis software, remeshing of the triangles was performed. The resulting mesh consisted of smoothed surfaces composed of reduced size equilateral triangles elements, with distorted elements appearing only in areas with sufficiently complex geometry. The edge lengths of these elements were set at 1 mm with a maximum edge length of 4 mm for the sharper elements. The setting of 1 mm was chosen based on the requirement that elements must also adequately represent the cortical bone thickness. Meshes were then exported as Abaqus/CAE software v6.6-1 (Simulia, Providence, RI) input files.

Soft tissues, such as the IVD, cannot be rendered properly in CT scans due to their low contrast. Thus, a different approach was used to include these regions in the model. Using Mimics, the discs were modeled with an intervertebral filler CAD solid body (cylinder), which was later reduced to the desired geometry by Boolean operations and by adjusting the peripheral vertical profile based on the upper and lower cross sectional areas of the vertebral endplates. The resulting body completely occupies the intervertebral volume, reflecting the in vivo placement of the IVD. The nucleus pulposus (NP) was then modeled by dividing the disc body with a cross sectional cutting profile in the superior-inferior direction. The profile was characterized taking into account anatomy. The IVD was now divided in two bodies, the NP and the annulus fibrosus (AF). The NP shares its external peripheral surface with the internal surface of the AF. External geometry meshes for the IVDs were also imported to the analysis software.

The simulation module in Mimics allows objects to be manipulated and repositioned in space. This tool allowed inspection for proper spine alignment and for flexibility in defining the posture of the subject. In this case standing, as opposed to a rest position in which the CT scan was taken.

### *B. Spatial Variations of Material density assignment*

Solid body meshing was performed with Abaqus based on the surface triangular mesh generated in Mimics. A tri to tetrahedral element conversion function was performed to define 4-node linear tetrahedral elements on the vertebral bodies. After this process, the volumetric meshes were then imported back into Mimics for density assignment. The purpose of this operation was to assign non-homogeneous material properties to account for varying bone density distribution. Multi-body FEA studies to date only model bone material properties based on a homogeneous two material distribution; a uniform block of cancellous bone surrounded by a cortical shell. On the other hand, a method that uses CT data to define material properties in a FE model may predict vertebral strength more accurately. Calculation of an interpolated HU value for each of the volumetric elements was performed. Due to the large number of elements for each vertebra and that this would had eventually resulted in thousands of material definitions in finite element model, the elements were grouped in a uniform distribution of 10 equally sized intervals in the -100 to 1400 HU range (10 different materials, number defined by taking into account characterization of cancellous bone using more than one material).

A study by Rho et al. demonstrated the use of CT values as predictors of mechanical properties of vertebral cancellous bone. Based on these results, a linear model was adopted in which CT values correlate with bone density in a linear regression equation. The curve was calibrated with the reported density values of $1.0\text{-}1.4\cdot10^{-6}$ kg/mm$^3$ for cancellous bone [3].

### *C. Hard Tissue Bone material assignment*

Both the cortical and the cancellous bone materials were defined as transversely isotropic (Table 1). This was modeled in Abaqus as orthotropic/elastic properties (engineering constants) by defining Young's modulus, Poisson's ratios and Shear modulus in the three principal directions. The posterior elements were defined as isotropic. As can be seen in Fig. 2, this is, to the best knowledge of the authors, the first multi-body model that incorporates a patient/specimen dependent CT-based spatial distribution of mechanical properties.

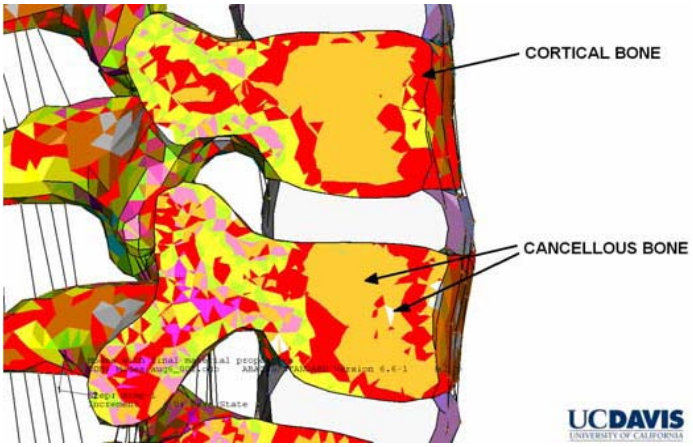


**Figure 2.** Sagittal cut at the pedicles showing material distribution

### *D. Soft-Tissue Modeling: Intervertebral discs and Ligaments*

The Intervertebral discs (IVD) is composed of an AF and a NP. These two bodies were assigned hyperelastic material properties. Hyperelastic materials are described in terms of a strain energy potential (per unit of reference volume). For the NP, a Mooney-Rivlin strain energy potential was selected with material parameters $C_{10}$ = 0.12, $C_{01}$ = 0.03 and $D_1$ = 0.00667 (Table 1). The parameter $D_1$ was set for a Poisson's number of

$\nu = 0.4995$.

Ligament properties were obtained based on existing scientific literature [5,12]. Force-displacement curves and stiffness tables were extracted from these references in order to describe the stiffness (N•mm-1) of the elements. Elements were modeled as tension-only axial cables with non-linear stiffness. This approach is adequate for cable-like ligaments (e.g. supraspinous ligament, SSL) and for membrane-like ligaments (e.g. anterior longitudinal ligament ALL) if cables are properly defined spatially in a serial-parallel arrangement

The seven ligaments (anterior longitudinal-ALL, posterior longitudinal-PLL, capsular-JC, flavum-LF, intertransverse-IT, interspinous-ISL and supraspinous-SSL) were modeled with different material properties for each set of two adjacent vertebral bodies: T12-L1, L1-L2, L2-L3, L3-L4, L4-L5 and L5-sacrum.

For the capsular ligament of the zygapophyseal joint, a bi-linear stiffness behavior (exponential-like behavior that "locks" the ligaments for values approaching 10 mm) was incorporated [5]. Also, the compressibility of articular cartilage and synovial fluid was considered [12]. This was modeled by incorporating the reported force-displacement curve into the compressive behavior of the axial element. Initial gap of the capsular elements depended on the particular joint but a 0.5 to 3 mm range was observed.

**Table 1** Material properties employed for the Finite Element Model

| Structure | Element Type | Young's and Shear Modulus (MPa) | Poisson's Ratio | Densities (kg/mm$^3$) | References |
|---|---|---|---|---|---|
| Cortical Bone | Transversely Isotropic C3D4 | $E_{xx}$ = 11,300 $E_{yy}$ = 11,300 $E_{zz}$ = 22,000 $G_{xy}$ = 3,800 $G_{yz}$ = 5,400 $G_{xz}$ = 5,400 | $\nu_{xy}$ = 0.484 $\nu_{yz}$ = 0.203 $\nu_{xz}$ = 0.203 | $1.8 \cdot 10^{-6}$ | Lu et al, 1996<br>Martin et al, 1998 |
| Cancellous Bone | Transversely Isotropic C3D4 | $E_{xx}$ = 140 $E_{yy}$ = 140 $E_{zz}$ = 200 $G_{xy}$ = 48.3 $G_{yz}$ = 48.3 $G_{xz}$ = 48.3 | $\nu_{xy}$ = 0.45 $\nu_{yz}$ = 0.315 $\nu_{xz}$ = 0.315 | $0.9\text{-}1.1 \cdot 10^{-6}$ | Lu et al, 1996<br>Martin et al, 1998<br>Rho et al, 1995 |
| Posterior Elements | Isotropic C3D4 | $E$ = 3,500 | $\nu$ = 0.25 | $1.4 \cdot 10^{-6}$ | Guo and Teo, 2005<br>Shirazi-Adl et al, 1986 |
| | | Hyperelastic Material Properties | | | |
| Annulus Fibrosus | Ogden N = 3 C3D4H | $\mu_i$ / $\alpha_i$: -8.72154 / 24.0609; 7.30044 / 25; 1.47347 / 19.113 | $D_1$ = 3.5 $\nu$ = 0.49 | $1.05 \cdot 10^{-6}$ | Guo and Teo, 2005<br>Wagner and Lotz, 2004 |
| Nucleus Pulposus | Mooney-Rivlin C3D4H | $C_{10}$ = 0.12 $C_{01}$ = 0.03 | $D_1$ = 0.00667 $\nu$ = 0.4995 | $1.02 \cdot 10^{-6}$ | Guo and Teo, 2005<br>Schmidt et al, 2007 |
| Ligaments | Axial Connectors CONN3D2 | non-linear force-displacement curves | | - | Eberlein et al, 2004<br>Kumaresan et al, 1998<br>Pintar et al, 1992 |

## COMPUTATIONAL MODEL VALIDATIONS

The model assumed an upper body weight of 30 kg with 80% of that weight redistributed at T12 as reported by Guo and Teo. Two types of analyses were performed on the model, natural frequency extraction up to the fifth mode and static loading in the form of pure flexion-extension and axial moments. Geometric nonlinearity was accounted for by performing a large scale displacement analysis. The moments were applied to the model at T12 via a simulated loading bar that mimics the in vitro loading. In this scheme, forces are defined so equivalent moments are applied at T12 upper surface. Increments were internally calculated by the software to achieve convergence. The final model was composed of 158,527 elements.

Boundary conditions for the model were set to constrain the six degrees of freedom at the nodes in the sacrum-pelvis joint.(Fig. 3)

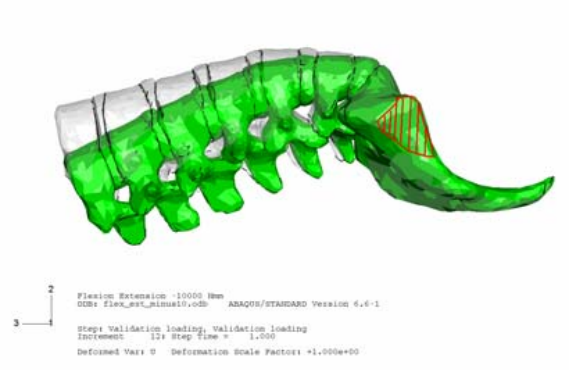

**Figure 3.** Flexion-extension displacements at -10 N·m (hatched zone shows fixed sacrum-pelvis joint)

*A. Response to static loading.*

The loading responses (angular deflection at T12) for flexion-extension and axial moments given by the present computational model were compared to in vitro testing by Panjabi et al. and Eberlein et al. (2004). The FE model results in our case exhibit similar behavior with the experimental data (Fig. 4) but the magnitudes are smaller in the case of flexion-extension and greater for axial moment loading. For the flexion-extension moment loading there is a non-linear and non-symmetric response as reported by the cited research but the stiffness is notably higher than the experimental results. This results in a response more flat than the compared angular displacement curves. For axial loading we have the opposite case whereas the response is far greater in magnitude (4x). General behavior matches in exhibiting a symmetric response.

*B. Modal response*

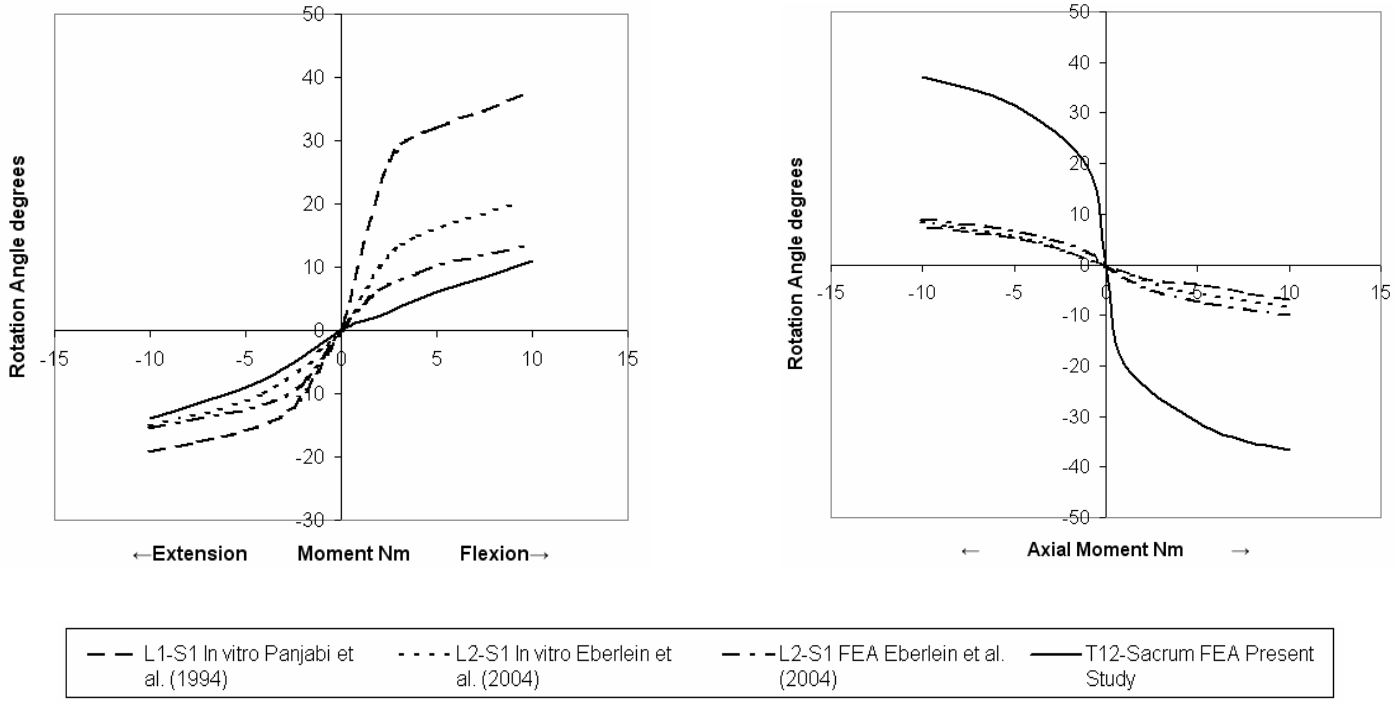


**Figure 4.** Flexion-extension and axial (torsion) moment loading results from the current FEA study versus 2- in vitro and 1 other FEA study results.

The first 5 frequencies and mode shapes were extracted from our analysis found to be within the 0-10 Hz ranges. Excellent correlations were obtained with values from literature that validates our model. The mode shapes are depicted in Figs. 5 to 7 and the numerical values are given in Table 2.

The first mode (resonant frequency = 0.41 Hz) corresponded to the anterior-posterior direction motion, similar to the expected results of an applied flexion moment. Displacement amplitudes of the eigenvectors were normalized to a maximum value of 1. As seen in Fig. 5, the maximum values are in the superior element, T12. The second mode (resonant frequency = 0.67 Hz) corresponds to a lateral bending-type deflection, Fig. 6. T12 was again the zone of the largest displacements. These first two modes showed the basic lumbar spine modes (resembling those consisting in static moment loading).

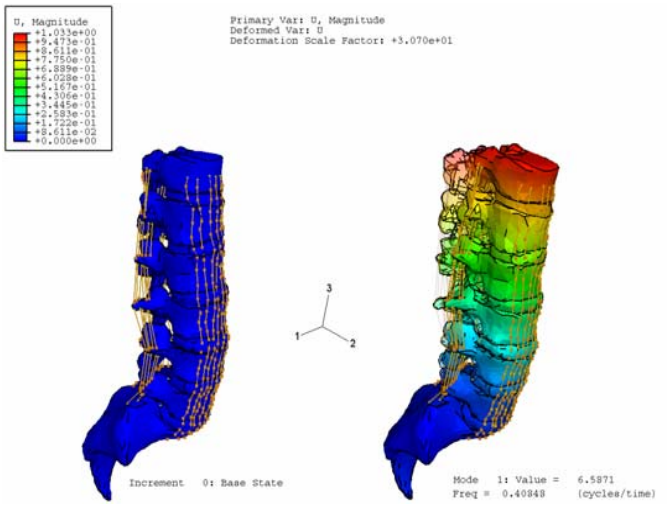


**Figure 5.** Base State and Mode 1 (A-P displacement).

The third mode was of particular interest. It consisted in a lordotic to straight lumbar spine curvature rearrangement. The frequency for this mode was 3.41 Hz. This "straightening up" of the spine results in an upward displacement of T12 and also a rotation that aligns T12 with the axial plane. Kitazaki and Griffin report that the upper body acts rigidly for this modal response so the eventual displacements that result from this rearrangement of the spine transmit up to the head. The resonant frequency for the fourth torsional mode was 3.66 Hz which is very close to the vertical vibration of the third mode. Finally, the fifth mode at 8.81 Hz (Fig. 7) resembles mode 3 but T12 dramatically rotates downwards, perhaps due to the distributed upper body weight conditions. The curvature of the lumbar spine changes to kyphotic for this mode.

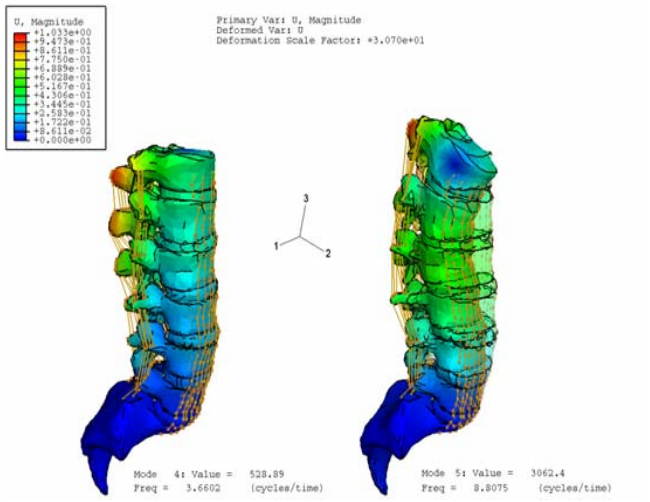


**Figure 6** Mode 2 (lateral displacement) and Mode 3 (straightening of the lordotic curvature)

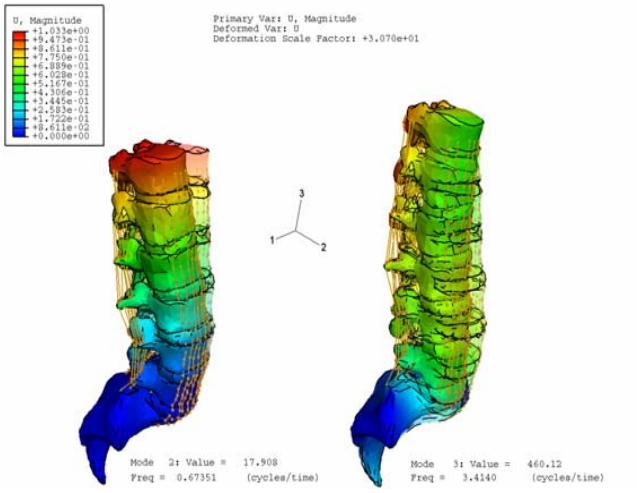


**Figure 7** Mode 4 (axial bending displacement) and Mode 5 (T12 rotation, change in lumbar curvature to kyphotic)

**Table 2** Frequency results and comparison with in vivo studies and available FEA solutions. Highlighted results represent in vivo studies for vertical resonance and the third mode for the present research

| Study | Type | Model | Mode shape | Resonant Frequency (Hz) |
|---|---|---|---|---|
| Pope and Hansson, 1992 | in vivo | – | "vertical resonance" | 4.6 |
| Kitazaki and Griffin, 1997 | in vivo | – | Mode 1 T1 A-P disp. | 1.1 |
| | | | Mode 2 | 2.2 |
| | | | Mode 3 | 3.4 |
| | | | Mode 4 whole body vertical disp. | 4.9 |
| | FEA 2-D | head to buttocks | Mode 1 A-P disp. of T12 (no sacrum disp.) | 0.28 |
| | | | Mode 2 | 1.49 |
| | | | Mode 3 | 2.81 |
| | | | Mode 4 lumbar disp. results in upper body vertical disp. | 5.06 |
| Kong and Goel, 2003 | FEA Sagittal plane restricted 3-D | head to sacrum ligamentous | Mode 1 A-P displacement | 0.43 |
| | | | Mode 2 | 2.79 |
| | | | Mode 3 | 5.34 |
| | | | Mode 4 vertical displacement | 8.32 |
| Guo and Teo, 2005 | FEA Full 3-D | T12 to pelvis ligamentous with 30 kg upper body weight | "vertical resonance" | 8.23 |
| Present Research | FEA Full 3-D | T12 to sacrum ligamentous with 30 kg upper body weight | Mode 1 A-P bending (no sacrum disp.) | 0.41 |
| | | | Mode 2 lateral bending | 0.67 |
| | | | Mode 3 straightening of spine, vertical disp. | 3.41 |
| | | | Mode 4 torsional, axial bending | 3.66 |

## CONCLUSION

An approach is developed in this paper for anatomically accurate performance predictions of human lumbar spine. It is shown that a CT examination scan can be employed to model a patient-specific high fidelity finite element analysis model. Bone density variations were taken into account. Although no direct assessment of the sensibility of the FEA with respect to varying bone density was studied, static loading results showed a similar trend with experimental results with similar spinal segment properties that validates our model. The difference in magnitudes is believed to be caused by the material property approximations of the IVD. There were no "calibration" process was conducted as there where no in vivo/vitro data to compare with (the CT scan belonged to a live person). Good correlation was obtained with experimental in vivo frequencies values, a first step in dynamic modeling of the human lumbar spine.

In summary, procedures developed in this work will serve useful in noninvasive evaluation of patients with back problems. The advantage of this approach is that the model can be tailored to specific individual or specimen.


## ACKNOWLEDEMENTS

The authors would like to thank Dr. Gupta, M.D. and Dr. Ramos-Grez, Ph.D. for their constructive comments. The authors greatly acknowledge the Materialise Company for making Mimics software available for the class.


## REFERENCES


[1] Goto, K., Tajima, N., Chosa, E., Totoribe, K., Kubo, S., Kuroki, H., Ara, T., 2003, "Effects of Lumbar Spinal Fusion on the Other Lumbar Intervertebral Levels (Three-Dimensional Finite Element Analysis)," Journal of Orthopaedic Science, 8(4), pp. 577–584.

[2] Rho, J.Y., Hobatho, M.C., Ashman, R.B., 1995, "Relations of Mechanical Properties to Density and CT Numbers in Human Bone," Medical Engineering Physics, 17(5), pp. 347-355.

[3] Martin, R.B., Burr, D.B., Sharkey, N.A., 1998, Skeletal Tissue Mechanics, Springer Verlag, New York.

[4] Panjabi, M.M., Oxland, T.R., Yamamoto, I., Crisco, J.J., 1994, "Mechanical Behavior of the Human Lumbar and Lumbosacral Spine as Shown by Three-Dimensional Load-Displacement Curves," The Journal of Bone and Joint Surgery, 76-A(3), pp. 413-424.

[5] Eberlein, R., Holzapfel, G.A., Fröhlich, M., 2004, "Multi-Segment FEA of the Human Lumbar Spine Including the Heterogeneity of the Annulus Fibrosus," Computational Mechanics, 34(2), pp. 147–163.

[6] Lu, Y.M., Hutton, W.C., Gharpuray, V.M., 1996, "Do Bending, Twisting, and Diurnal Fluid Changes in the Disc Affect the Propensity to Prolapse? A Viscoelastic Finite Element Model," Spine, 21(22), pp. 2570-2579.

[7] Guo, L., Teo, E., 2005, "Prediction of the Modal Characteristics of the Human Spine at Resonant Frequency Using Finite Element Models," Proceedings of the Institution

of Mechanical Engineers Part H: Journal of Engineering in Medicine, 219(4), pp. 277-284.
[8] Shirazi-Adl, A., Ahmed, A.M., Shrivastava, S.C., 1986, “Mechanical Response of a Lumbar Motion Segment in Axial Torque Alone and Combined with Compression,” Spine, 11(9), pp. 914–927.
[9] Wagner, D.R., Lotz, J.C., 2004, “Theoretical Model and Experimental Results for the Nonlinear Elastic Behavior of Human Annulus Fibrosus,” Journal of Orthopaedic Research, 22(4), pp. 901-909.
[10] Schmidt, H., Heuer, F., Drumm J., Klezl, Z., Claes, L., Wilke, H.J., 2007 “Application of a Calibration Method Provides More Realistic Results for a Finite Element Model of a Lumbar Spinal Segment,” Clinical Biomechanics, 22(4), pp. 377–384.
[11] Kumaresan, S., Yoganandan, N., Pintar, F.A., 1998, “Finite Element Modeling Approaches of Human Cervical Spine Facet Joint Capsule,” Journal of Biomechanics, 31(4), pp. 371-376.
[12] Pintar, F.A., Yoganandan, N., Myers, T., Elhagediab, A., Sances JR, A., 1992, “Biomechanical Properties of Human Lumbar Spine Ligaments,” Journal of Biomechanics, 25(11), pp. 1351-1356.
[13] Pope, M. H., Hansson, T. H., 1992, “Vibration of the Spine and Low Back Pain,” Clinical Orthopaedics & Related Research, 279(6), pp. 49-59.
[14] Kitazaki, S., Griffin, M.J., 1997, “A Modal Analysis of Whole-Body Vertical Vibration, Using a Finite Element Model of the Human Body,” Journal of Sound and Vibration, 200(1), pp. 83-103.
[15] Kong, W.Z., Goel, V.K., 2003, “Ability of the Finite Elements Models to Predict Response of the Human Spine to Sinusoidal Vertical Vibration,” Spine, 28(17), pp. 1961-1967.